



Assessment of water resources setting using hydrogeochemistry and geophysics study El-Tur area, South Sinai Governorate, Egypt

Moustafa M. Abo El-Fadl^{1*}, Abdel-Hameed M. El-Aassar¹, Mohamed A. Khaled²

1-Hydrogeochemistry department, Egyptian Desalination Research Center of Excellence (EDRC), Desert Research Center, El-Matrayia, Cairo, Egypt, B.O.P. 11753, Egypt.

2- Geophysics department, Desert Research Center, El-Matrayia, Cairo, Egypt, B.O.P. 11753, Egypt.

*Corresponding author, e-mail: mmaboelfadl@hotmail.com : 202-01003450013

Abstract

Due to the sustainable development importance of El-Qaa Plain, El-Tur area, a geophysical and hydro-geochemical study was carried out. The main aquifer in the study area is Quaternary.

23 Vertical Electrical Sounding stations were conducted. There are two dry geoelectric layers. The third and fourth layers are the upper and lower part of the aquifer.

The collected 58 groundwater samples were evaluated for different purposes. Total dissolved salts ranged from 303 to 3835 ppm. 83% of groundwater samples are suitable for irrigation purposes according Na%. Also, 93% of total groundwater samples lie in good water class.

Key words: Geophysics, Hydrogeochemistry, Groundwater evaluation, El-Tur area

Received; 29 April 2018, Revised form; 23 May 2018, Accepted; 23 May 2018, Available online 1 July. 2018

1. Introduction

Sinai Peninsula is an important part of the Egyptian territories as it represents about 6% of the total area of Egypt. It enjoys a unique geopolitical location. In the same time, it is becoming increasingly clear that in view of the present population growth rate in Egypt, the reclamation of more and more desert areas is an important prerequisite to face the food problem for the present and next coming generations.

The study area occupies the middle part of El-Qaa plain, where previous exploratory works have revealed that the Post Miocene sediments have its maximum thickness including an aquifer with a reasonable thickness, relatively shallow depth to water and moderate water quality.

El-Qaa plain is served by a good road system that links it to most parts of Sinai as well as Suez and Cairo. Most of the works carried out in this area with the purpose of studying its water resources was on an exploratory level, while works that are more detailed needed to plan for the development of the area, based on its groundwater resources.

Therefore, the main objective of the present work is to study and evaluate the Quaternary aquifer in the middle part of El-Qaa plain in a more detailed way than that carried out before. This is important to avoid the results based on interpolation between the relatively few locations on which previous studies have been based, and to come up with a more realistic picture about the groundwater resources of the area. This would be achieved through the following:

- 1- Recognizing the Geology of the area in view of the previous geological works.
- 2- Carrying out a detailed geoelectric resistivity survey covering the area of study.

- 3- Interpretation of the geoelectric measurements to determine the aquifer geometry and characteristics.
- 4- Using the available data of some drilled wells such as electric logs, lithologic logs, and pumping test data and its relation to the concluded geoelectric parameters to evaluate aquifer potentialities.
- 5- Collecting water samples from the drilled wells for chemical analysis to evaluate its water quality for different uses.
- 6- Representing the results in the form of tables, diagrams, maps and cross sections.
- 7- Recommending –within the study area- the sites of relatively high developmental potential based on groundwater resources.

El-Qaa plain occupies the southwestern part of Sinai Peninsula and is lies between the latitudes 28° 00' and 28° 50' N and longitudes latitudes 33° 20' and 34° 00' E and cover about 15 km², Fig.(1). It is mainly covered by sedimentary deposits.

The climatic conditions play an important role in studying, analyzing and interpreting the geomorphological characteristics, as well as, the hydrogeological conditions. El-Qaa plain is an arid area where, from the available meteorological data, the mean maximum temperature is 34.8°C during August while the mean minimum temperature is 8.9°C during February. The highest humidity is about 64% during September while the minimum value is 58% during March. Such humidity is mainly due to the effect of the Gulf water. The maximum amount of rainfalls is about 11 mm/year. The maximum amount for one day is about 31 millimeters, [2, 3].

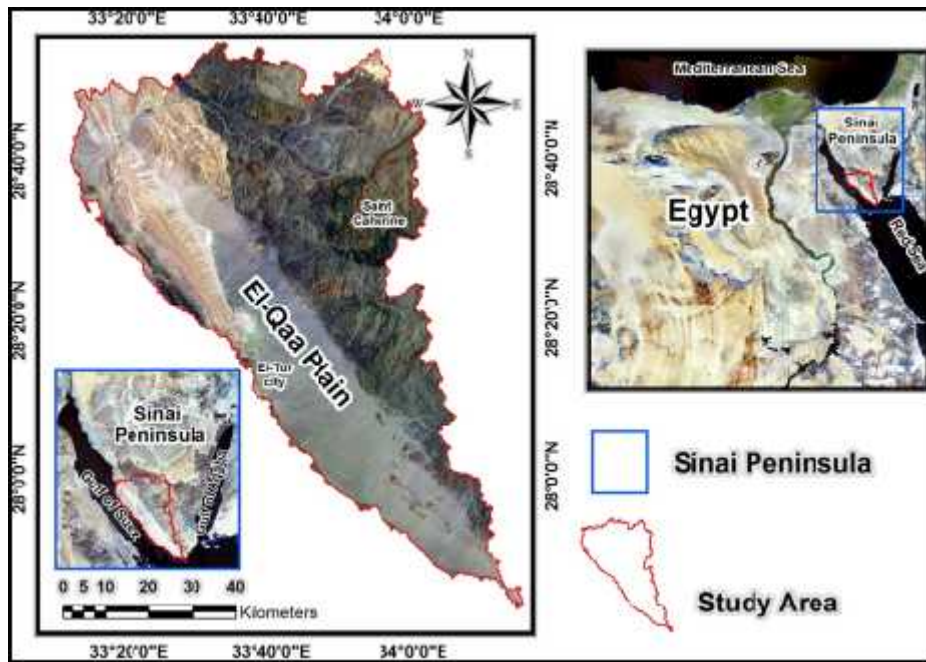


Fig (1): Location map of El-Qaa Plain area, southwestern Sinai, Egypt (Landsat ETM), after [1].

2. Topography and geology of the study area.

Topographically, El-Qaa plain, as a whole, is one of the major and conspicuous topographic and geomorphic landforms in the eastern shoulder of the Gulf of Suez, Fig. (2).

It represents a structural depression trending in a NW-SE direction, parallel to the mean Clysmic rift and extending for about 150 km, from Wadi Firan in the north to Ras Mohamed in the south, with a mean width of about 15km. It is an extensive gravelly plain, characterized by its closed shape in the north and is surrounded by the high

mountains of basement rocks in the east which rise to 2,662 m asl at Gabal Katherine and the sedimentary rocks of Gebel Qabeliat in the west which are generally between 200 and 300 m asl and composed of different sedimentary units and basement rocks. Due to the south, it is replaced by several hillocks, such as Gebel Abu Swiera and Gebel Hamam Saydna Mousa. The elevation of the plain varies from zero to 200 m asl and consists of wadi deposits, rock fragments, alluvium deposits (sand and gravel), sabkha and playa Fig. (2).

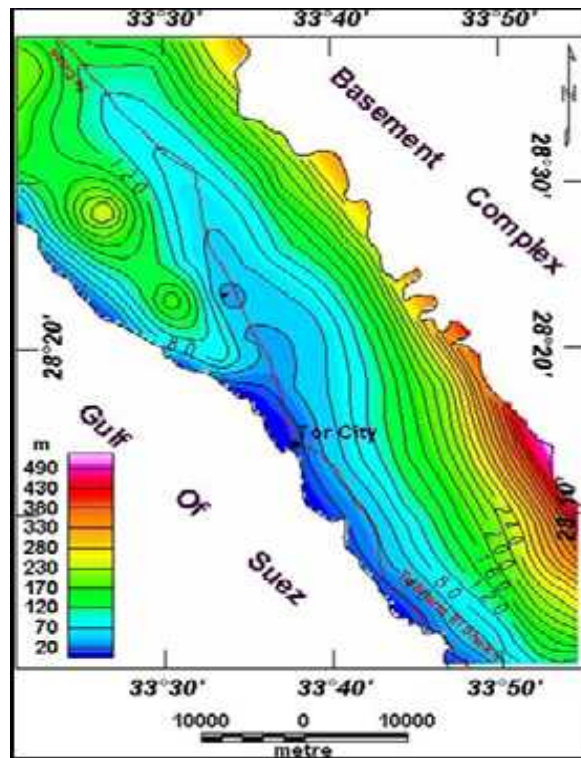


Fig (2): Topographic map of the El Qaa plan area [2]

3. Geologic setting:

El-Qaa plain is an extensive gravelly plain stretching in NE-SW direction. It is covered mainly by the Quaternary deposits. In the east the Pre-Cambrian granites, metamorphic and the old Carboniferous clastics bound it. In the west, it is bounded by Eocene limestone and Miocene limestone and gypsum forming Gebel Qabaliat ridges. Rocks belonging to the Upper Tertiary are also present on the surface of the area. The rocks outcropping in the study area, as shown in the geological map, Fig. (3), reflect the different geologic periods ranging from the Pre-Cambrian to the Quaternary.

Granites are mainly of the syn-tectonic type and are highly intruded by dikes along fracture lines. Dikes are of acidic and basic types and stand in relief, due to their high resistance to erosion. The granitic rocks also form the uplifted Gebel Araba mass in the western portion of the study area, in which joints are more frequent and dikes are less observed.

The most well developed sedimentary section is found at Gebel Araba, starting from the Carboniferous, which is mainly formed of dark sandstones. Cretaceous sandstone follows up in the section. It comprises shale and limestone

beds. This is followed up by the Paleocene strata, which are mainly formed of shale and chalky limestone. Eocene limestone capes the underlying formations. It is further followed upward in some parts by the Miocene shale, marl and limestone. Evaporites, assigned to the Miocene period, are also outcropping in the low-lying areas.

The Quaternary aquifer consists of gravel, sands, clays and sandy clays and is considered the main sediments composing the plain area.

To the south of the line joining El-Tur town and the mouth of Wadi Shidding, the deposits can be divided into two distinct groups; the eastern group and the western group. The eastern group is made up mainly of fluvatile and subordinately lacustrine and marine sediments, while the western is marine. Near the eastern hills, the sandy clay gives place to sand and gravel that gradually become coarser until they change to granite and other igneous boulders mixed with wind-blown sand. To the west, between El-Tur and Gebel Hamam Sayedna Mousa, the ground is covered by silty clay. Gebel Hamam Sayedna Mousa and El Araba range consist of Nubia sandstone and Cretaceous marls capped by a bed of crystalline limestone.

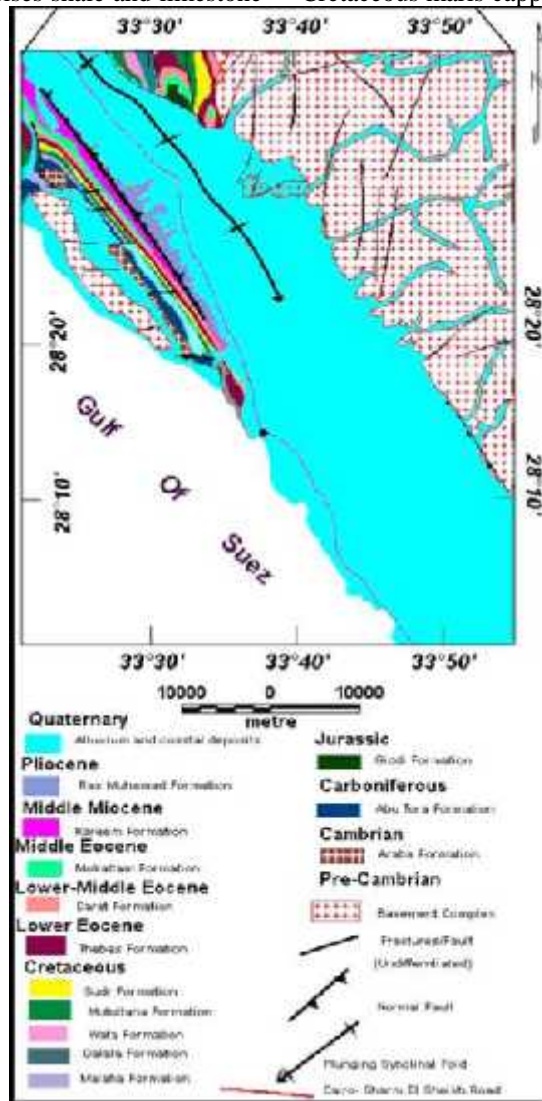


Fig (3): Geologic map of El-Qaa plain showing different lithological units.

4. Hydrogeologic setting:

1-The groundwater in southern Sinai is mainly associated with the wadi fill with fractured igneous rocks and at depth ranging from 2 to 25m.

2- The Quaternary aquifer at El-Qaa plain north of El-Tur consists of gravels, silts and clay with cobbles and boulders of basement rocks. Local rainfall contributes to the recharges of this aquifer.

3- The aquifer thickness exceeds 1000m and is recharged by runoff from the adjacent upland area. The average annual precipitation in El-Qaa Plain is less than 80 mm with a notable increase towards the east of the study

area [1]. The southern Sinai massif receives more than average precipitation of 65–100mm annually, Fig. (4). The precipitation comes almost exclusively in winter and sometimes occurs as snow on the high peaks, whereas convective rains occur during all seasons, causing flooding in the study area [4]. The hydrographical basins of El-Qaa Plain have high surface and groundwater potentialities due to the eastern branches of their steep sloping channels draining from the highlands of south and central Sinai where high rates of rainfall prevail.

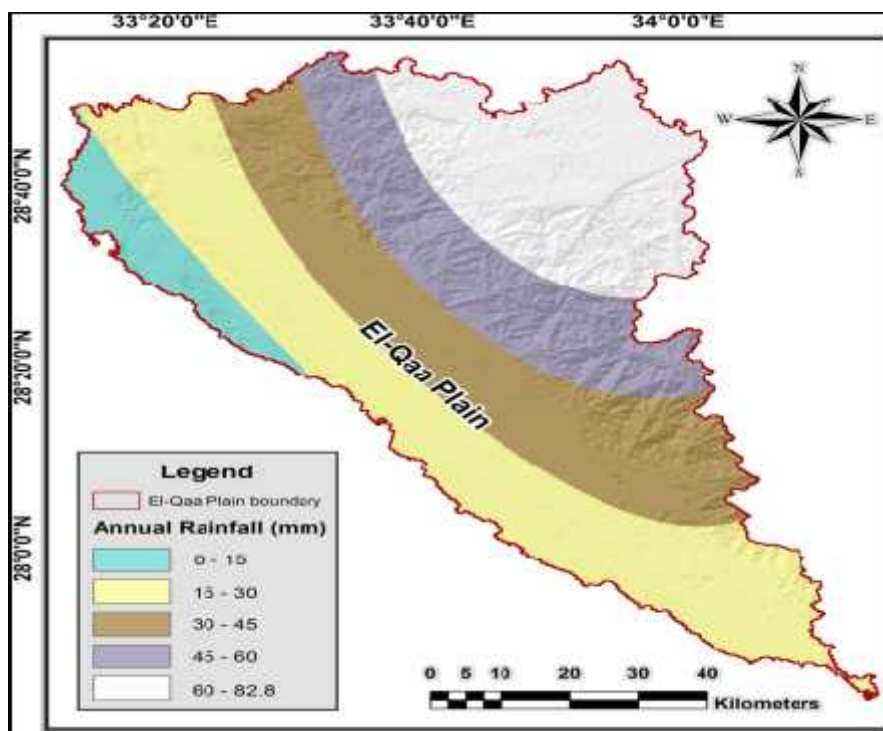


Fig (4): Rainfall map showing average annual precipitation of El-Qaa plain [1].

5. The field works:

5.1. Vertical electrical resistivity sounding survey:

A vertical geoelectric soundings (23 VES) were carried out in the area Fig. (5), five of which were selected to be beside water wells whose well logging, lithologic and hydrogeologic data are available to get correlation between the measured sounding curves and the corresponding key layers. The sounding stations were distributed, such that to provide reasonable coverage for the study area.

The Schlumberger electrodes configuration was applied with current electrode distance (AB) started with two meters and increase progressively to reach 1000 m or 2000m at El Wadi area. The geoelectric measurements were carried out using the resistivity meter SAS 1000. The instrument measures the apparent resistance (R) with high accuracy. Using the Schlumberger's formula, the apparent resistivity (ρ_a) was calculated at every value of AB/2. At each sounding station, the electric resistivity was

measured against half the current electrode spacing in the form of field resistivity sounding curve. The measured resistivity (apparent resistivity in $\Omega \cdot m$) reflects the type of rock penetrated by the electric current, while half of the electrode spacing is an expression of the depth of the penetrated rock layer. The calculated apparent resistivity values (ρ_a) were plotted against half current electrodes spacing (AB/2) on logarithmic scale each cycle, 6.25 Cm as V.E.S curves.

The locations of the Vertical Electric Sounding (VES) stations were tentatively located on the topographic map (scale 1: 100000). In the field, topographic land survey was carried out in order to determine the accurate locations and the ground elevations of the sounding stations Fig. (5). Use a Global Positioning System (GPS) model "GARMIN" beside conventional land survey devices. To have some of these stations beside wells or bore holes already existing in the area for the purpose of correlating geophysical data with geological ones.

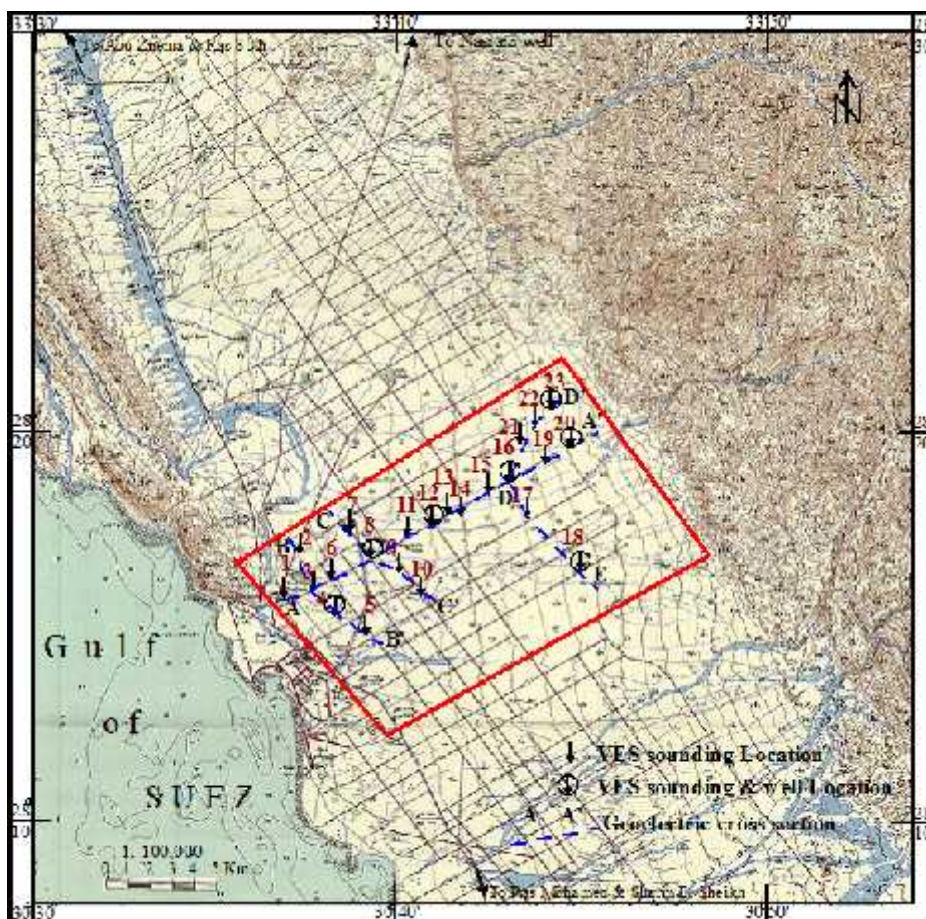


Fig (5): Location map of the sounding stations in the study area.

5.2. Sampling and water analysis

Based on the different activity in the area, total groundwater samples 58 were collected from irrigation groundwater (41 samples) and drinking groundwater (17 samples) used in the middle part of El Qaa Plain El-tur area in August 2015, Fig. (6), and table (1).

The locations of the sampling sites were recorded using Garmin GPS. Polypropylene bottles (500 ml) using them for sampling purpose. These dried bottles were carried to field and were used during the collection of water samples from each site, [5, 6].

Table (1): Chemical analysis of major cations and anions of the groundwater samples of irrigation and drinking water in El Tur area.

samples No	pH	EC	TDS	Na ppm	Ca ppm	Mg ppm	K ppm	HCO ₃ ppm	SO ₄ ppm	Cl ppm	CO ₃ ppm
Irrigation. Groundwater samples											
1	7.4	2043	1193	110	240.0	47.3	5	27.5	213.6	554.5	9.0
2	7.1	2145	1310	240	164.0	32.6	3	58.0	385.0	455.9	0.0
3	7	6390	3835	650	439.9	160.5	7	76.3	1110.0	1429.4	0.0
4	7.4	2442	1456	280	200.0	29.3	3	27.5	256.0	665.4	9.0
5	8	1271	769	160	98.1	7.6	3	30.5	180.0	295.7	9.0
6	7.7	813	442	96	63.6	3.0	2	76.3	36.9	202.1	0.0
7	7.4	1468	882	195	106.6	8.7	2	64.1	212.8	325.3	0.0
8	7.4	918	557	92	88.1	13.0	3	45.8	106.0	231.7	0.0
9	7.4	857	473	104	60.0	3.6	2	39.7	64.0	216.9	3.0
10	7.4	881	506	92	74.6	10.3	3	30.5	70.0	231.7	9.0
11	7.5	3690	2078	200	491.4	27.8	5	36.6	297.4	1035.1	3.0
13	7.6	785	455	93	59.3	4.6	3	54.9	130.0	138.0	0.0
14	7.5	923	532	92	80.7	11.7	4	45.8	94.0	226.7	0.0
15	6.7	2568	1493	160	300.0	38.6	5	48.8	373.7	591.5	0.0
16	7.6	916	531	124	60.3	3.2	2	42.7	140.0	177.4	3.0
19	6.6	704	381	98	40.1	2.4	2	61.0	45.0	162.7	0.0
20	7.3	722	417	92	50.7	3.5	2	58.0	72.0	167.6	0.0

samples No	pH	EC	TDS	Na ppm	Ca ppm	Mg ppm	K ppm	HCO ₃ ppm	SO ₄ ppm	Cl ppm	CO ₃ ppm
21	6.9	1055	600	95	102.1	7.7	3	61.0	150.0	212.0	0.0
22	7.5	1534	894	120	167.7	12.4	3	45.8	195.0	369.7	3.0
23	6.9	1015	553	73	101.9	7.1	7	45.8	146.6	192.2	3.0
25	7.2	1090	627	73	127.9	11.3	3	42.7	172.5	212.0	6.0
26	7	2576	1511	140	320.0	41.1	4	54.9	362.5	616.1	0.0
27	6.8	1128	632	75	115.3	19.0	2	51.9	183.2	212.0	0.0
28	6.8	648	356	68	53.3	5.5	2	45.8	58.6	142.9	3.0
30	6.8	2257	1260	140	237.0	44.3	4	48.8	240.0	566.8	3.0
33	6.7	804	459	72	77.2	12.1	3	58.0	88.0	177.4	0.0
34	6.6	2122	1221	250	118.4	37.6	4	61.0	325.0	455.9	0.0
35	7.1	1317	802	145	126.0	6.6	3	45.8	175.0	320.4	3.0
36	7.2	898	505	72	85.8	12.4	3	42.7	110.0	197.2	3.0
38	6.7	1003	594	80	100.0	17.4	3	48.8	137.5	231.7	0.0
40	7.4	847	512	104	69.8	1.8	2	51.9	140.8	167.6	0.0
42	7.1	552	303	60	42.5	4.9	2	61.0	40.0	123.2	0.0
44	6.8	2789	1642	140	345.0	56.1	3	39.7	400.0	677.7	0.0
46	7.2	650	382	68	55.1	9.2	2	45.8	82.0	142.9	0.0
47	6.6	669	365	64	50.2	9.6	2	51.9	80.0	133.1	0.0
55	7.3	1377	757	155	110.1	6.4	1	51.9	150.0	308.1	0.0
56	5.7	801	448	64	85.0	11.8	2	295.9	39.0	98.6	0.0
57	7.1	920	500	84	81.7	11.9	2	42.7	62.4	236.6	0.0
58	7.2	906	534	84	88.9	12.8	2	45.8	82.0	241.5	0.0
59	6.9	667	379	70	56.3	6.5	2	51.9	50.9	167.6	0.0
60	7.1	681	373	68	57.3	7.0	2	54.9	43.4	167.6	0.0
min	5.7	552.0	303.1	60.0	40.1	1.8	1.0	27.5	36.9	98.6	0.0
max	8.0	6390.0	3835.0	650.0	491.4	160.5	7.0	295.9	1110.0	1429.4	9.0
average	7.1	1410.8	817.5	127.8	131.5	19.0	3.0	55.3	178.1	328.7	1.7
Drinking groundwater samples											
12	7.6	2375	1397	310	124.8	42.1	5	48.8	355.0	529.9	6.0
18	7	722	448	104	48.2	1.9	2	48.8	134.0	133.1	0.0
24	6.9	1208	700	130	110.2	2.4	2	48.8	181.6	246.5	3.0
29	7.1	1023	564	125	72.2	3.5	2	48.8	130.0	207.0	0.0
31	7.2	648	319	60	45.9	5.9	2	54.9	61.0	113.4	3.0
32	7.1	654	345	68	50.6	5.8	2	45.8	69.0	123.2	3.0
37	6.4	1917	1071	110	206.2	33.9	3	45.8	325.6	369.7	0.0
39	7	783	398	90	55.5	2.2	1	67.1	30.7	182.4	3.0
41	6.9	806	492	76	76.1	12.5	2	27.5	140.0	162.7	9.0
43	7.2	652	346	66	48.0	7.7	2	54.9	52.5	133.1	9.0
45	6.6	752	376	72	56.0	7.7	2	61.0	40.0	167.6	0.0
48	6.9	670	366	60	55.5	9.5	2	51.9	80.0	133.1	0.0
49	7.1	672	378	60	59.6	9.2	2	54.9	84.0	133.1	3.0
50	6.9	670	377	58	60.7	8.2	2	61.0	85.0	133.1	0.0
51	7.3	701	412	70	59.1	10.6	2	45.8	90.0	157.7	0.0
52	6.9	1055	618	105	97.9	10.0	2	45.8	134.0	246.5	0.0
53	7	936	515	100	70.8	8.5	2	42.7	130.0	182.4	0.0
min	6.4	648	318.61	58	45.85	1.908	1	27.45	30.68	113.369	0
max	7.6	2375	1397.1	310	206.2	42.07	5	67.1	355	529.876	9
average	7.0	955.5	536.5	97.8	76.2	10.6	2.17	50.23	124.8	197.30	2.29
Sea	8.1	61300	42203	11950	597.6	1415	230	95	4525	22616	21
Rain	7.9	117	68	6.6	15.1	1.5	1	27.6	6.4	23.1	0

EC and pH were measured on site using respective electrodes. The physical and chemical parameters were determined using the following standard protocol given by the American Public Health Association [7]. Bicarbonate and chloride were analyzed using titration methods; sulfate

was analyzed using double beam UV–Vis spectrophotometer following APHA. Sodium and potassium were analyzed by Flame photometer, while calcium and magnesium were analyzed using Thermo-Scientific ICP spectroscopy.

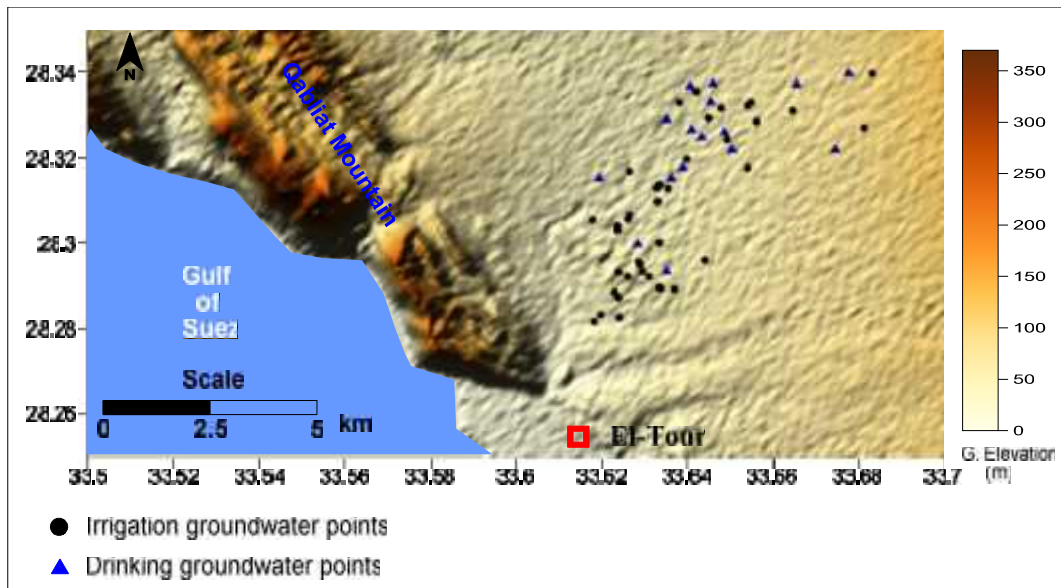


Fig (6): Locations map of representing groundwater of the Quaternary aquifer in El Qaa plain area.

6. Discussion of the geoelectrical results:

The Quantitative interpretation of the filed curves revealed that the geoelectrical succession is formed of a number of layers, as follows:

1- There is no sharp lithologic change along the investigated depth. Consequently, the discrimination between the successive geoelectrical layers is governed mainly by other factors such as the water content, nature of the surface cover and quality of water.

2- The main geoelectrical succession consists of two distinguished sections; an upper dry section and a lower water-bearing section. The dry section is further divided into an upper "surface" layer having higher resistivity due the nature of the surface rock type and a lower one having less, but more uniform resistivity. The water bearing section is divided into upper and lower layers. The lower layer differs from the upper one in that the salinity of water is possibly higher and/or the clay content is larger.

3- The aquifer extends downward beyond the investigated depth and consequently the bottom of the aquifer is not reached. This means that the aquifer thickness is more than what can be concluded from the present work, although the water quality deteriorates downwards due, to the seawater intrusion.

Geoelectrical cross sections constructed along specific profiles were selected to express the two-dimensional variation of resistivity and thickness with depth along reasonably distributed traverses. One geoelectrical cross section is selected to find out the corresponding variations along the NE-SW direction, Fig. (7). However, three other cross sections are constructed in the N-S direction, i.e. perpendicular to the direction of the first set, to detect any possible variation along that direction, while the last geoelectrical profile NE-SW Figs. (8 &9).

To avoid repetition in description of these cross sections, a general description is given as to the

distribution of the four main geoelectrical layers, including the water-bearing formation as follows:

1- The first Zone: The first geoelectrical zone consists of upper surface dry sand and gravel intercalated with clay, derived from the eastern sedimentary and igneous hills, of recent deposits, with resistivity ranges from 356 to 2554 $\Omega \cdot m$. Its thickness increases towards the east, varies along this direction for few meters.

2- The second Zone: This Zone consists of sand and gravel intercalated with clay of dry Quaternary deposits, with resistivity ranges from 54 to 87 $\Omega \cdot m$. Its thickness increases towards the east due to the rising of ground surface, which ranges between 25 and 45 m.

3- The third Zone: The third geoelectrical layer is the water-bearing formation with a resistivity ranging between 16 and 64 $\Omega \cdot m$ and thickness ranging from 57 to 85m. It consists of sand and gravel intercalated with clay of Quaternary deposits saturated with fresh to slightly brackish water, and its thickness increases towards the east, Figs. (9 &10).

4- The fourth Zone: The fourth geoelectrical zone consists of sand, gravel and clay of Quaternary deposits with brackish water. The resistivity of this layer is generally low and varies within a narrow range (5-9 $\Omega \cdot m$).

The thickness of this zone was not identified as it represents the last detected layer in the geoelectrical succession. The depth to the interface increases towards the SW direction. It has to be mentioned that due to the vertical lithologic similarity of the Quaternary deposits in the study area, the distinction between the upper part of the water-bearing formation and the lower part is based mainly on the water quality as reflected by the electric resistivity ranges.

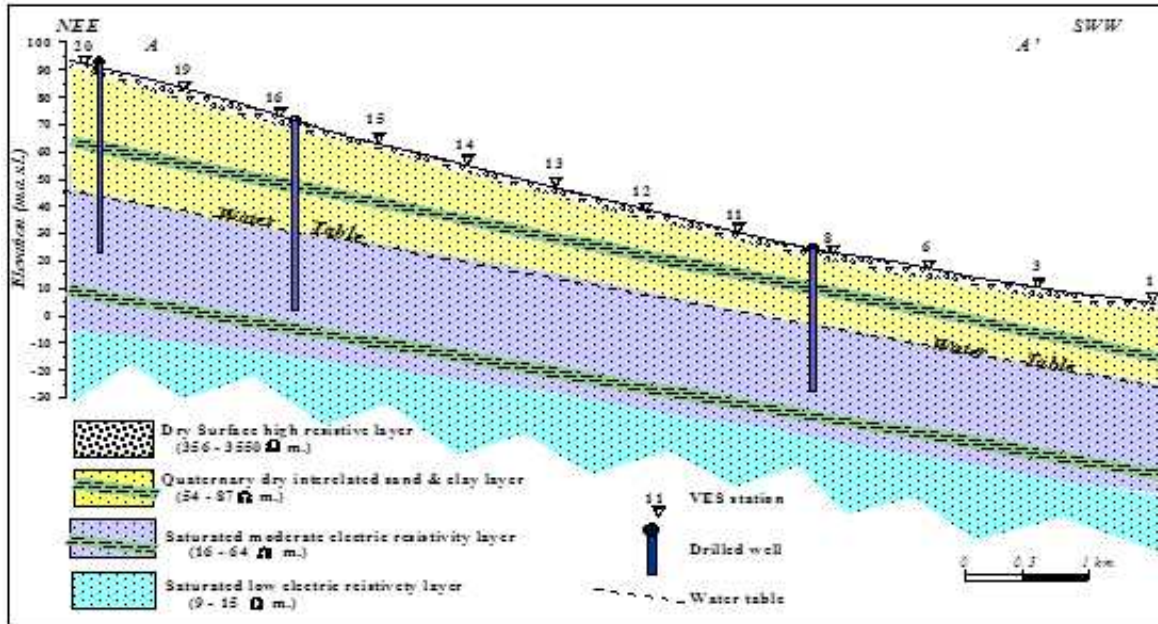


Fig (7): Geoelectrical cross section A-A' (in El Wadi area).

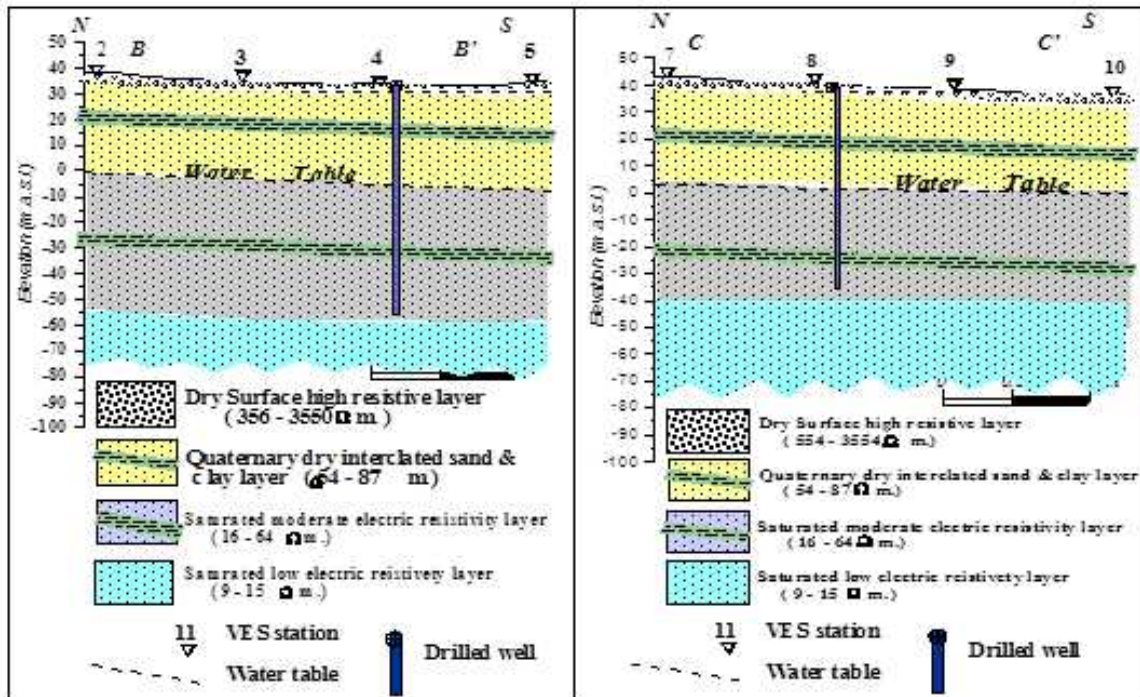


Fig (8): Geoelectrical cross sections BB' & C-C' (in El Wadi area).

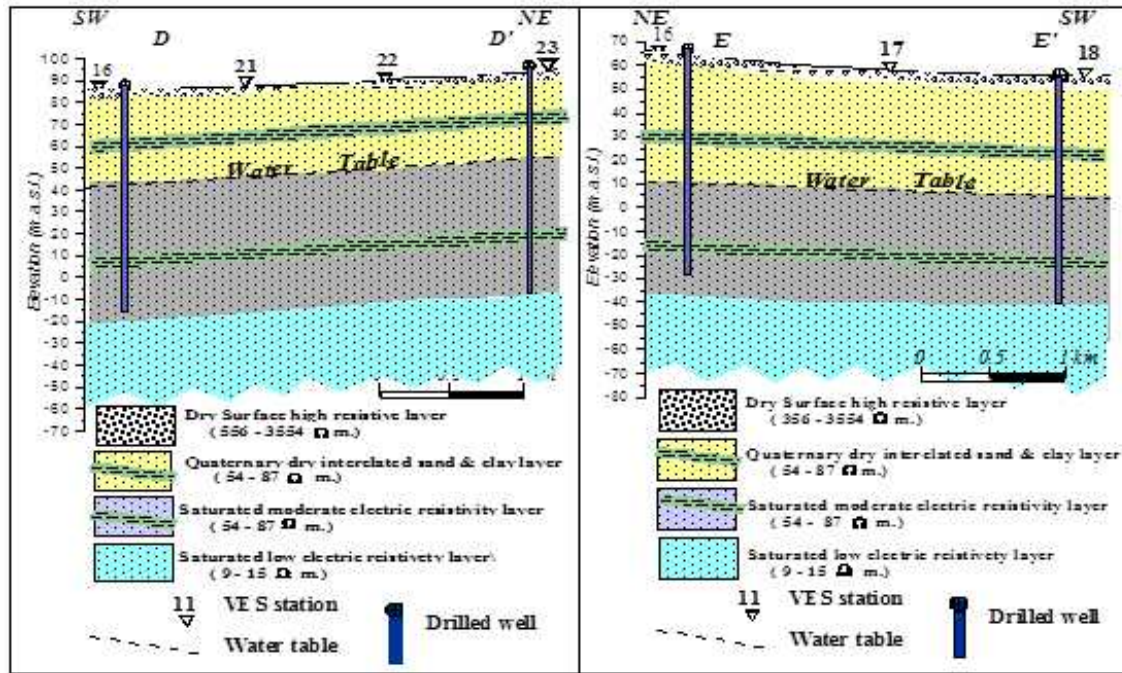


Fig (9): Geoelectric cross section D -D' & E- E' (in El-Wadi area).

7. Hydrogeochemical results:

7.1. Groundwater chemistry:

The values of pH ranged from 5.7 to 8.0 with an average value of 7.1 for irrigation groundwater samples. While the pH of drinking groundwater samples was varying between 6.4 and 7.6 with an average value of 7.01. This reflects that pH of groundwater in the study area is neutral.

Electrical conductivity of the irrigation groundwater samples varies from 552 to 6390 $\mu\text{s/cm}$ with an average value 1410 $\mu\text{s/cm}$. Also, electrical conductivity of the drinking groundwater samples varies from 648 to 2375 $\mu\text{s/cm}$ with an average value 955 $\mu\text{s/cm}$.

Total dissolved solid of the irrigation groundwater samples varies from 303.1 to 3835 mg/l (av. 817.5mg/l). While, total dissolved solid of the drinking groundwater samples varies from 318.6 to 1397mg/l with an average value 536.6mg/l. The salinity is increased towards southwest direction from recharged of local rainfall and surface runoff contributes from the adjacent upland area due to the Quaternary aquifer at El-Qaa plain in the north direction consists of gravels, silts and clay with cobbles and boulders of basement rocks. So, the chemical characteristics of groundwater of the Quaternary aquifer in El-Tur area may be affected by the Miocene limestone and anhydrite exposures of Gebel Qabaliat.

7.2. Total hardness:

The hardness values of drinking water ranged from 128 to 654 with average value 234 mg/l as CaCO_3 . On the other hand, the TH of irrigation water ranged from 110 to 1759 with average value 406 mg/l as CaCO_3 . The classification of groundwater based on total hardness (TH) shows that the majority of the irrigation water are more than 200mg/l as CaCO_3 .

7.3. Alkalinity:

The alkalinity values of drinking water ranged from 35.0 to 60 with an average value 45.0 mg/l as CaCO_3 . On the

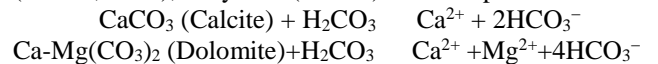
other hand, the alkalinity of irrigation water ranged from 32.5 to 242.7 with an average value 48.2 mg/l as CaCO_3 . The classification of groundwater based on alkalinity shows that all of the drinking and irrigation water are less than 200mg/l as CaCO_3 except sample No.56.

7.4. Major ions distributions:

64.7% of samples are $\text{Na}^+ > \text{Ca}^{2+} > \text{Mg}^{2+}$ with $\text{Cl}^- > \text{SO}_4^{2-} > \text{HCO}_3^-$ and $\text{Cl}^- > \text{HCO}_3^- > \text{SO}_4^{2-}$, while 35.3% of samples are $\text{Ca}^{2+} > \text{Na}^+ > \text{Mg}^{2+}$ with $\text{Cl}^- > \text{SO}_4^{2-} > \text{HCO}_3^-$ in drinking groundwater samples. But in irrigation groundwater samples, 56.1% are $\text{Na}^+ > \text{Ca}^{2+} > \text{Mg}^{2+}$ with $\text{Cl}^- > \text{SO}_4^{2-} > \text{HCO}_3^-$ and $\text{Cl}^- > \text{HCO}_3^- > \text{SO}_4^{2-}$, while 43.9% of water samples are $\text{Ca}^{2+} > \text{Na}^+ > \text{Mg}^{2+}$ with $\text{Cl}^- > \text{SO}_4^{2-} > \text{HCO}_3^-$. According to Schoeller 1977 [8], the sequence of cations shows matrix water origin affected by leaching and dissolution of water bearing rocks.

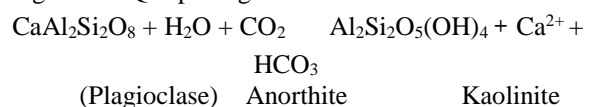
7.4.1. Calcium (Ca) and magnesium (Mg):

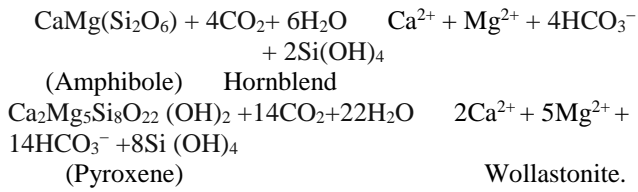
The original source of Ca^{2+} & Mg^{2+} ions are dissolving calcite (CaCO_3), magnesite (MgCO_3) and dolomite ($\text{Ca-Mg}(\text{CO}_3)_2$) from carbonate rocks beside gypsum ($\text{CaSO}_4 \cdot 2\text{H}_2\text{O}$), anhydrite (CaSO_4) from evaporites.



The increasing of Ca^{2+} & Mg^{2+} concentration in the area of study as revealed from the hydro-chemical coefficients: $\text{Ca}^{2+}/\text{Mg}^{2+}$, $\text{Ca}^{2+}/\text{SO}_4^{2-}$, $\text{Ca}^{2+}/\text{Ca}^{2+} + \text{SO}_4^{2-}$, $\text{Ca}^{2+}/\text{HCO}_3^-$, $\text{Ca}^{2+}/(\text{HCO}_3^- + \text{SO}_4^{2-})$, $\text{Ca}^{2+}/(\text{Ca}^{2+} + \text{Mg}^{2+})$ and $\text{Mg}^{2+}/(\text{Ca}^{2+} + \text{Mg}^{2+})$, they show that there are other sources of Ca^{2+} & Mg^{2+} beside carbonates minerals and evaporites.

1-The hydrolysis of feldspars, amphibole and pyroxenes are important sources of increasing Ca^{2+} & Mg^{2+} in El Qaa plain groundwater.





Also, Calcium and magnesium ions are significant to appraise the magnitude of seawater influence [9]. The estimate of average value of Ca/Mg ratios are 7.3 and 6.4 in drinking and irrigation groundwater indicating completely in the budget of Ca and Mg due to interaction with rocks and arid climate conditions of the area, Fig (10). The Ca+Mg vs HCO₃ range between 0.4 to 33.9 with an average 7.2 in irrigation groundwater but in drinking groundwater, it ranged between 1.7 to 12.3 with an

average 3.7. The high value in irrigation groundwater is due to long distance of subsurface movement of water through aquifer matrix. Figure (11) shows the Ca²⁺+Mg²⁺ vs HCO₃⁻ in the drinking and irrigation groundwater in study area. Increasing in concentration of Ca+Mg ions against decreasing in concentration of HCO₃ is due to leaching and dissolution of carbonate and dolomite rocks. The Ca and Mg are mainly driven from the weathering of ophiolites with influence of carbonate rocks. Han and Lie, 2004 [10], have used the variables in the composition of water Mg/Ca vs Na/Ca to distinguish limestone, dolomite and silicate rock sources of ions. The groundwater samples plots close to igneous rocks with influence of carbonate rocks.

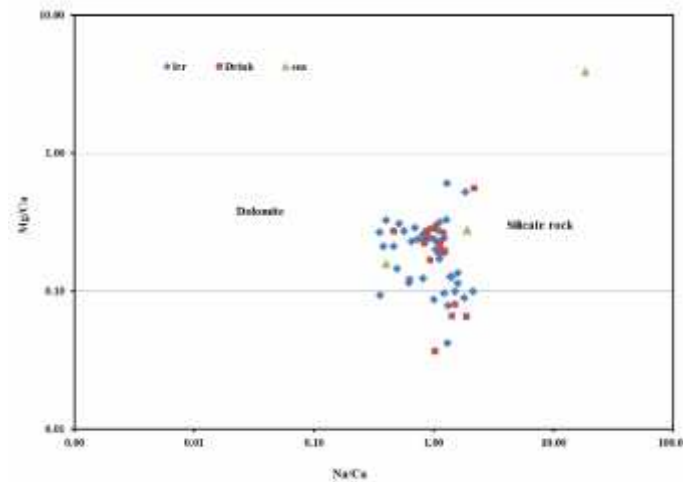


Fig (10): Mg/Ca vs Na/Ca of irrigation and drinking groundwater in El Tur area.

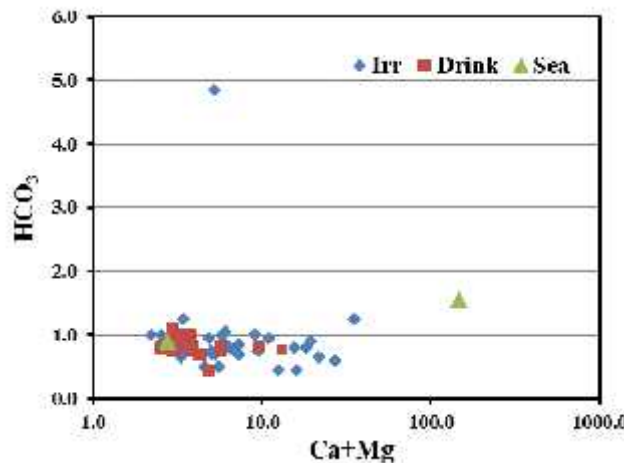


Fig (11): HCO₃ vs (Ca+Mg) of irrigation and drinking groundwater in El-Tur area.

7.4.2. Sodium and potassium:

The original source of Na⁺ and K⁺ ions are dissolution of halite (NaCl) and sylvite (KCl) minerals. The increasing concentration of Na⁺ and K⁺ ions in the area of study as revealed from the hydro-chemical coefficients Na/(Na+Cl) or (Na+K)/(Na+Cl) more than 0.5 (Hounslow, 1995), (Table 1) and increasing (Na&K) in the ratios Na/K, Na/Ca, (34% of samples is <1 and 66% >1), Na/Mg and Na/HCO₃. (Na+K)/(Ca+Mg), all these ratios indicate other sources of Na ions than halite.

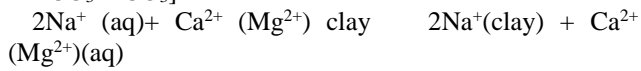
The other sources of Na⁺ & K⁺ ions are declared as follows:

Aghazadeh and Mogaddam, 2010 [11] described Chloro-alkaline indices (CAI 1, 2) to show the change in chemical composition of groundwater during its travel in the subsurface. When there are cations exchange of sodium and potassium from water with magnesium and calcium in the host rock, the exchange is known as direct, (indices are positive) if the indices are negative, the

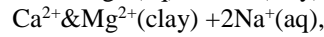
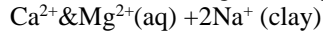
exchange is reversed and indirect indicating chloro-alkaline disequilibrium [8, 12].

$$\text{(Chloro Alkaline Indices) (CAI-1) = [Cl-(Na+ K) /Cl]}$$

$$\text{(Chloro Alkaline Indices) (CAI-2) = [Cl_-(Na+K)]/ SO_4 +HCO_3+ CO_3]}$$



Reverse ion exchange and depletion of Na⁺



Direct ion exchange depletion of Ca²⁺& Mg²⁺ and enrichment of Na⁺

The ion exchange processes between (Na&K) and (Ca&Mg) are declared also by Na⁺/Ca²⁺ and Na⁺/Mg²⁺ ratios.

The statistics of CAI 1, 2 of the samples of study area indicates 93.2% of the groundwater samples have positive

values and 6.8% are negative values in irrigation groundwater, while the samples of drinking water have 94.2% positive and 5.8% negative values, Fig. (12).

It simply implies that all groundwater of irrigation and drinking have suffered from ion exchange between alkali and alkaline earth metals. This explains the reason for the abundance of alkalis in the groundwater over alkaline earth elements. Cation exchange is possible when exchange sites such as clay minerals are present. Clay minerals are the product of silicate weathering [13, 14]. Thus, enhancing the ion-exchange process of the chloro-alkaline index values of the groundwater samples from the study area indicates base exchange reaction.

Figure (13), shows the process of ion exchange Ca/Ca+SO₄ ratio is further supported from low average value 0.7 and 0.62 for irrigation and drinking groundwater respectively, [15].

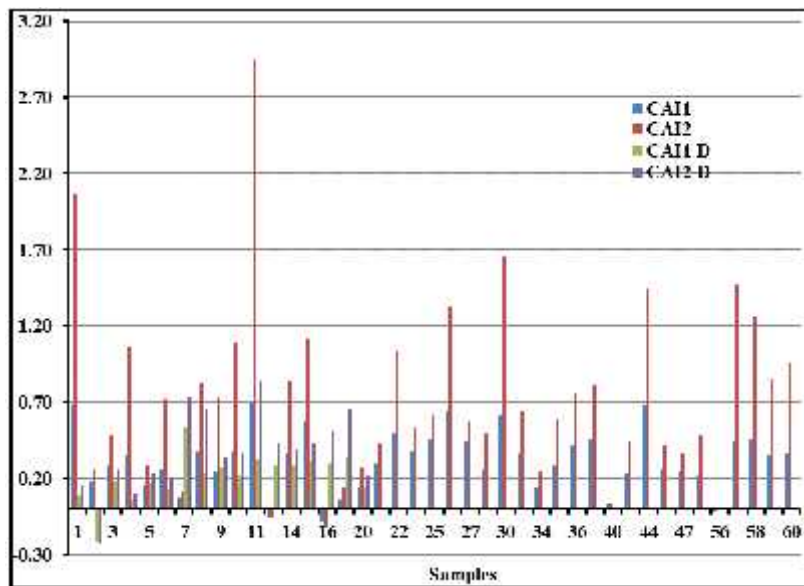


Fig (12): CAI-1 and CAI-2 of irrigation and drinking groundwater in El Tur area.

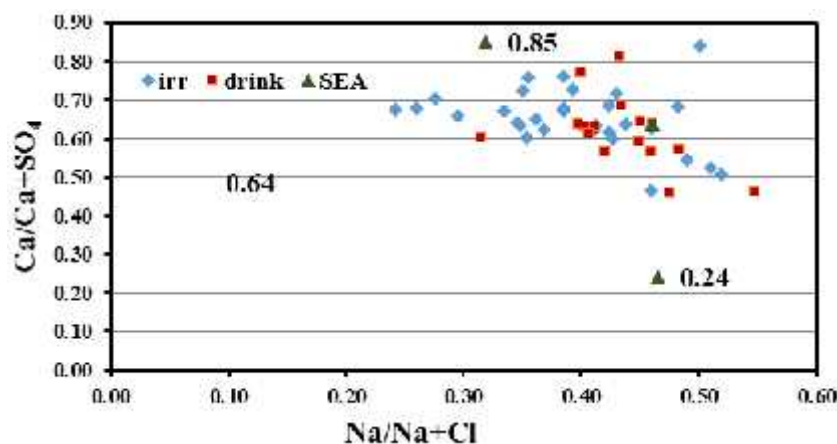


Fig (13): Ca/Ca+SO₄ vs Na/Na+Cl of irrigation and drinking groundwater in El Tur area.

7.4.3. Na vs. Ca ratio:

In Na vs. Ca scatter diagram Fig. (14), all of the irrigation and drinking groundwater samples fall on the aquiline, showing equal concentration of Ca and Na. This

further strengthens the support for ion exchange process in the study area. Ion-exchange process may be responsible for higher concentration of Na in groundwater.

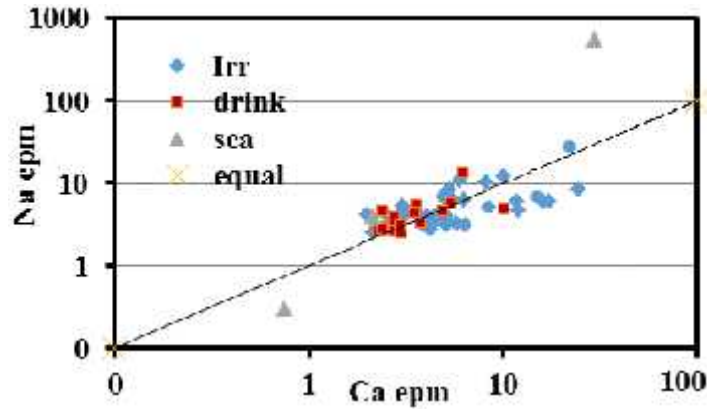


Fig (14): Na vs Ca of irrigation and drinking groundwater in El Tur area.

7.4.4. Carbonate & bicarbonates, chlorides, and sulfates:

Chloride is widely distributed in the groundwater in El Qaa area, the order of anions is $Cl^- > HCO_3^- > SO_4^{2-}$. Chloride represents 45% of total anions and its concentration ranges between 98.6 mg/l and 1429 mg/l with mean value of 306mg/l, and SO_4^{2-} ranges between 30.7mg/l and 1110mg/l with mean value of 176mg/l. The carbonate and bicarbonates concentration ranges between 27.5 mg/l and 297 mg/l with mean value 59 mg/l.

The hydro-chemical coefficients reveal the enrichment of chlorides in the groundwater of El Qaa area. K^+/Cl^- & Na^+/Cl^- & Mg^{2+}/Cl^- & Ca^{2+}/Cl^- & SO_4^{2-}/Cl^- & Cl^-/HCO_3^- & HCO_3^-/Cl^- and HCO_3^-/Cl^- . $Cl^-/total\ anions$ [15].

Reverse all coefficient $Cl^-/(HCO_3^- + CO_3)$ in meq/l ranges between 0.57 and 41.72 with mean value of 9.92 i.e. highly contaminated with saline water [16].

The sources of chloride in groundwater are (NaCl) and (KCl) salts; it constitutes approximately 0.05% of the lithosphere. The chloride-bearing minerals occurring in igneous rock are the feldspars ($Mal\ (Al,\ Si)_3O_8$), where $M=Fe,\ Sr,\ Rb,\ Ba,\ Ca,\ Na,\ K$.

Non cyclic sulfate (NCS) = $(Cl/7.2) - SO_4$ in mg/l ranges between -911.47 and -5.37 with mean value -133.37, negative value means that the principal source of SO_4 ions are minerals of terrestrial source as evaporites (gypsum, anhydrite and epsomite).

Also, Todd, 1959 [16] categorized groundwater according to HCO_3^-/Cl^- ratio as:

1- Normal good groundwater, i.e. not contaminated (less than 1).

- 2- Slightly contaminated water (more than 1 and less than 2).
- 3- Moderately contaminated water (2-6).
- 4- Seriously contaminated water (more than 6 and less than 15).
- 5- Highly contaminated water (more than 15).

All drinking water samples are normal good groundwater, i.e. not contaminated (less than 1) and all groundwater samples for irrigation except No.56. This is due to the low concentration of HCO_3^- and high concentration of Cl from leaching and dissolution of marine facies of water shed area.

In the scatter diagram of $(Ca + Mg)$ vs. $(HCO_3^- + SO_4)$, Fig. (15), the samples falling above the equiline (1:1), represent carbonate weathering (dissolution of calcite, dolomite, and gypsum) and reverse ion exchange as dominant processes; while samples falling below the equiline indicate the silicate weathering and ion exchange within the area [17, 18]. In the present study, most of the irrigation groundwater samples are present above the equiline Fig. (15), indicating that the carbonate weathering and reverse ion exchange processes are governing processes, while some of the samples fall below the equiline due to an excess of bicarbonate, which indicate that silicate weathering and ion exchange are also occurring. In other hand, the drinking groundwater samples fall around the equiline indicate that direct and reverse ion exchange processes at the same time.

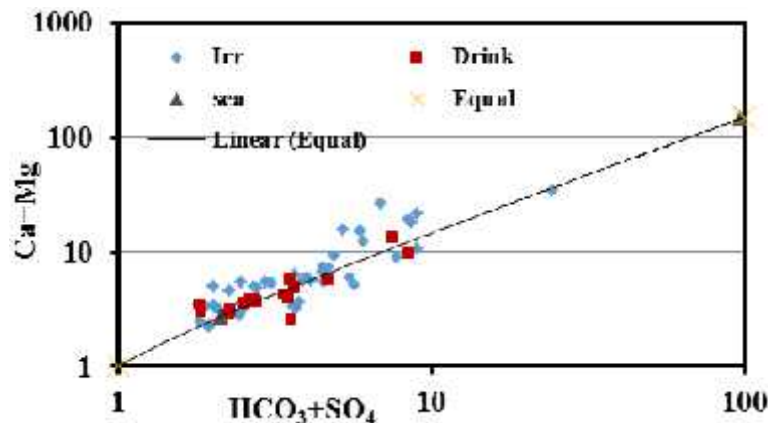


Fig (15): $(Ca+Mg)$ vs $(HCO_3^-+SO_4)$ of irrigation and drinking groundwater in El Tur area.

Increase in alkalis ions Na+K with the simultaneous increase of Cl⁻ + SO₄ Fig. (16), indicates a common source of these ions, resulting from dissolution of soil salts [19,

20]. Excess of Na over K is observed due to the greater resistance of K to chemical weathering [21].

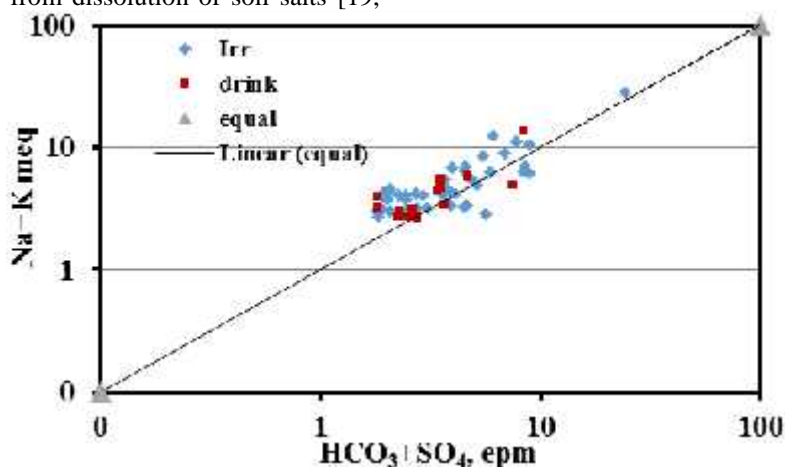


Fig (16): (Na+K) vs (HCO₃+SO₄) of irrigation and drinking groundwater in El Tur area.

REX factor calculates the salinization of the groundwater expressed as $\{(Na + K+Mg \text{ in meq/l}) - 1.076 *Cl\}$. From Table 1, some groundwater samples (10.3%) have the negative values indicating salinization in these groundwater samples, which are mainly affected by Gulf of Suez water and suffering seawater intrusion, while 89.7% have the positive value indicates fresh ground water intrusion.

8. Groundwater suitability

Groundwater chemistry can be utilized to evaluate water quality for different purposes [22, 23]. In addition, sodium and bicarbonate in the area indices like SAR and sodium % have been used to determine its suitability for agricultural purposes.

8.1. Drinking water quality

The analytical results of physical and chemical parameters of groundwater were compared with the standard guideline values as recommended by the World Health Organization for drinking purposes [24]. According to the standard limits of WHO [24], the data show that, 64.7% of drinking groundwater and 31.7% of irrigation groundwater are suitable for drinking proposes where TDS less than 500ppm. While the evaluation of the groundwater for drinking according Chebotarev, 1955 [25], all drinking groundwater samples are suitable. On the other hand, 91.3% of irrigation groundwater samples are suitable and 9.7% of groundwater samples are unsuitable for drinking proposes where the guideline is less than 1500ppm.

8.2. Suitability of the water for irrigation proposes

The groundwater concentrations were interpreted and calculated with irrigation indexes using the following formula as follows:

- Sodium percentage (Na %)
- Sodium absorption ration (SAR)
- Residual sodium carbonate (RSC)
- Magnesium Absorption ratio (MAR)
- Kelley's Ratio (KR)

8.2.1. Wilcox's classification (1955)

Wilcox classification [26], suggested the definition of sodium percentage relative to common cations percentage in the following equation:

$$Na\% = Na^+ \times 100 / (Ca^{2+} + Mg^{2+} + Na^+)$$

Where cations concentrations are in meq/l. This classification is based on the relation between sodium and salinity governing the suitability of waters for irrigation. For irrigation groundwater of study area, 39% of total groundwater samples are located in excellent to good class. Other groundwater samples 41% are located in good to permissible class while the rest of groundwater samples (20%) are located in doubtful to unsuitable class. In drinking groundwater samples of study area, 65% of total groundwater samples are located in excellent to good classes. Other groundwater samples 29% are located in good to permissible classes while the few groundwater samples (6%) are located within the doubtful to unsuitable classes, Fig. (17).

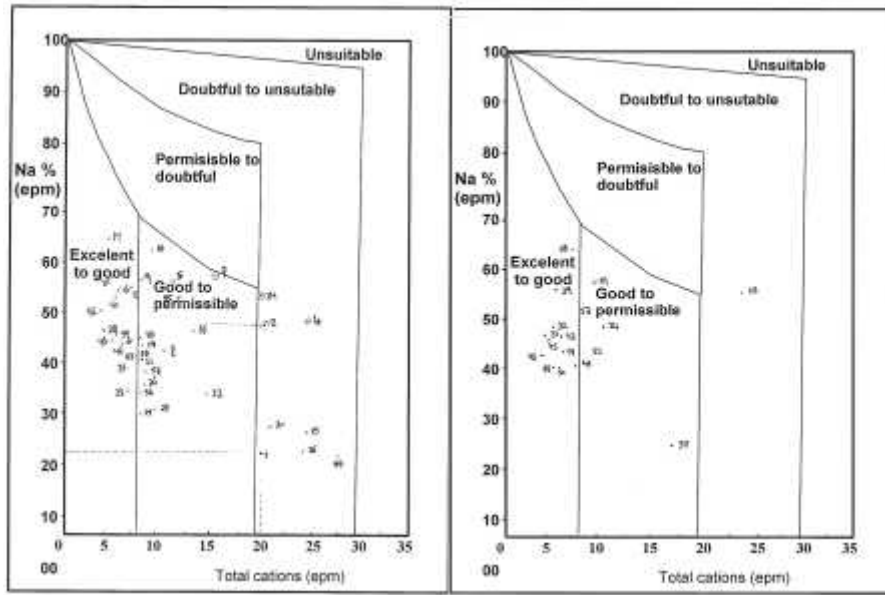


Fig (17): Classification of groundwater for irrigation purposes according to Wilcox method in El Tur area.

8.2.2. The U.S. salinity laboratory classification:

This classification is based essentially on salinity and sodium adsorption ratio (SAR). According to this classification $SAR = Na^+ / \{0.5(Ca^{2+} + Mg^{2+})\}^{0.5}$ [27].

Where Na^+ , Ca^{2+} , Mg^{2+} are in meq/l. High values of SAR imply a hazard of sodium replacing adsorbed Ca^{2+} and Mg^{2+} and this replacement causes damaging of soil structure. A nomogram is widely used for the evaluation of waters for irrigation purposes. This nomogram consists of a plot of specific conductivity (in $\mu mhos/cm$) which is a function of the dissolved solids concentration against SAR.

Applying this classification to the irrigation groundwater samples (41 samples) and drinking

groundwater samples (17 samples) in the studied area leads to the following, table (1), Fig. (18).

Salinity and SAR of major groundwater samples of irrigation groundwater in El Tur area indicate good water class represented by 19.5%, 63.5% and 9.6% for (C₂-S₁), (C₃-S₁) and (C₄-S₁) respectively, while 7.4% of water samples represent moderate water class (C₄-S₂). In addition, the majority of groundwater samples of drinking water lies in good water class as 53% and 41% for (C₂-S₁) and (C₃-S₁). Moreover, the 6% of drinking groundwater lies in (C₄-S₂). It is clear that the majorities of all groundwater samples (93%) are apparently suitable for irrigation and lie in good water class.

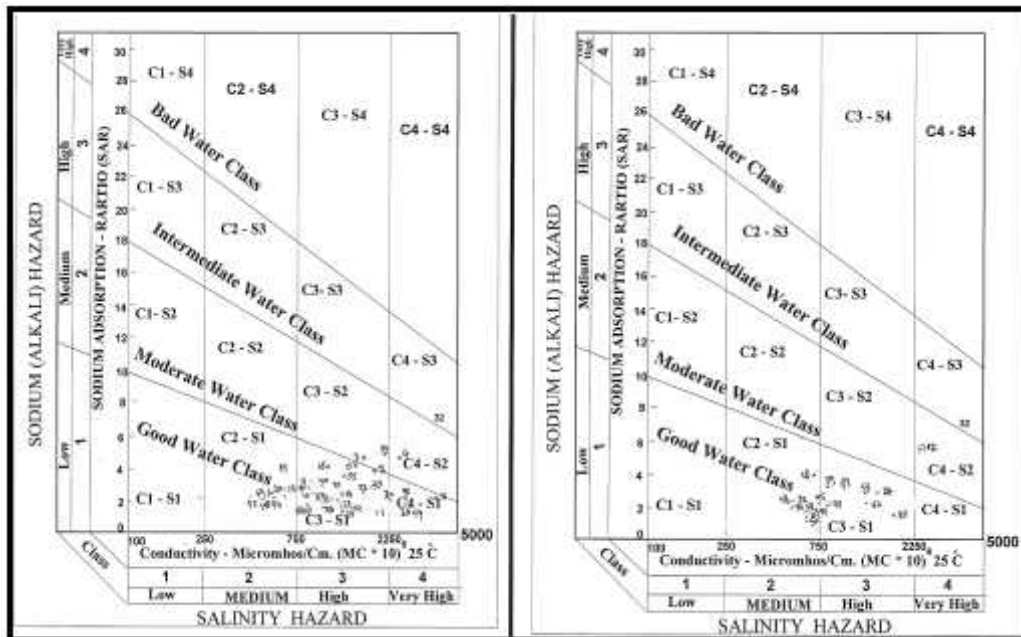


Fig (18): Diagram for the classification of irrigation water in El Tur area.

8.2.3. Residual sodium carbonate

To determine the hazardous effect of carbonate and bicarbonate on the quality of water for agricultural purposes, evaluation of residual sodium carbonate is important. RSC considers the excess concentration of bicarbonate and carbonate over the sum of calcium and magnesium. RSC has been calculated by following equation [28]:

$$RSC = (CO_3^{2-} + HCO_3^-) - (Ca^{2+} + Mg^{2+})$$

Where, all ionic concentrations are expressed in meq/l, (Eaton, 1950).

According to the classification scheme for RSC [29], all samples fall under the good category having RSC below 1.25 meq/l. This means that, the water type is soft. The high value of RSC in water may lead to the increase in the adsorption of sodium in the soil [30]. In groundwater having a higher concentration of bicarbonate, calcium and magnesium have the tendency to precipitate, and this causes the dissolution of organic matter into the soil.

8.2.4. Magnesium absorption ratio (MAR)

Generally, alkaline earths are in equilibrium state in groundwater. If more magnesium is present in waters, it affects the soil quality converting it to alkaline and decreases crop yield. Szabolcs and Darab, 1964 [31] proposed magnesium hazard (MH) value for irrigation water as given:

$$MH = Mg / (Ca + Mg) \times 100$$

Where concentrations in meq/l. $MH > 50$ is considered unsuitable and harmful for irrigation purpose. Generally, drinking groundwater samples range from 3.5 to 35.7 % with an average 16.9 % meq/l and irrigation groundwater range from 4 to 37.6% with an average value 16.6 %. The spatial distribution of magnesium hazard in groundwater as shown in Fig. (19) indicates that, all groundwater samples are within the range less than 50 % reflecting its suitability for irrigation uses

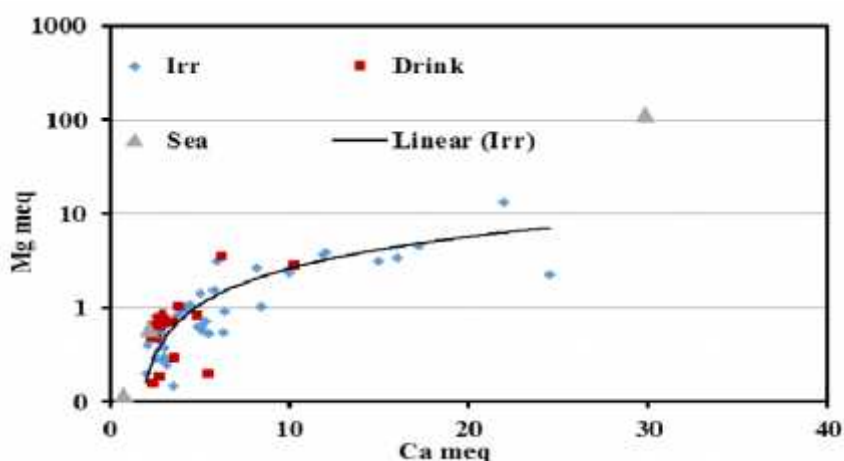


Fig (19): Magnesium hazard for drinking and irrigation groundwater samples of El Tur area.

8.2.5. Kelley's Ratio (1940)

Sodium measured against Ca^{2+} and Mg^{2+} is used to calculate by (Eq.) (Kelley, 1940) [32].

$$KR = Na / (Ca + Mg) \quad \text{as meq/l}$$

Where all the ion concentrations are expressed in meq/L. A Kelley's index (KI) of more than unity indicates an excess level of sodium in waters. Therefore, water with $KI (<1)$ is suitable for irrigation, while those with $KI (>1)$ is unsuitable [33]. In the present study area, KI values varied from 0.3 to 1.9 with average value 0.9 in drinking water. While in irrigation groundwater, it ranged from 0.36 to 1.77 with an average value 0.97 (Table 1). According to Kelley's index, 70.5% of drinking and 70.7 % of irrigation groundwater samples are suitable for irrigation, 29.5, and 29.3% of drinking and irrigation groundwater samples are limited for irrigation system.

Conclusion and recommendations:

The study area is locating at northeast El-Tur city and covering an area of about 15 km². The collected groundwater (58 samples) used for drinking, domestic and irrigation purposes. The aquifer is recharged by runoff from the adjacent upland area. 23 vertical Electric

sounding (VES) stations were conducted. The quantitative interpretation for the field curves was carried out using a computer program RISIST. Five geoelectric cross sections were constructed from the interpreted geoelectric data, from top to base.

The dry surface lay in the first and second. However, the third geoelectric layer is the upper part of the water-bearing formation and consists of gravel and sand with some clay intercalations. While the fourth geoelectric layer is the lower, part of the water bearing formation and has less resistivity than the upper part. It is saturated with brackish water. According to the ground elevation, depth to water and the depth to the interface of the fresh-brackish water, hand dug wells can be dug in the western part near the coast, while the drilling wells can be drilled in the eastern part. The depth to water from analysis of geoelectric data is ranging between 25 and 45 m, and water table ranging from 16 to 22 m.a.s.l.

The eastern part of the study area is the best site for drilling new wells, because it has suitable thickness of the water-bearing formation.

Pumping rate should be controlled to obtain the highest well efficiency and well specific capacity with less well loss and aquifer loss. The suitable well design must be used with appropriate pumping rate. It must be taken in consideration that the depth of new drilled wells do not exceed the depth of the upper surface of the fourth geoelectric layer, to avoid penetrate the saline water bearing zone.

Acknowledgement

The authors acknowledge the financial support for this work from the Science and Technological Development Fund (STDF) in Egypt through Grant 5240 (Egyptian Desalination Research Center of Excellence, EDRC).

References

- [1] S.M. Abuzied, H.A. Alrefae, "Mapping of groundwater prospective zones integrating remote sensing, geographic information systems and geophysical techniques in El-Qaa Plain area, Egypt" *Hydrogeol J* 25 (2017) 2067–2088.
- [2] S. A. Sultan, M. I. Mohameden, F. M. Santos, "Hydrogeophysical study of the El Qaa Plain, Sinai, Egypt" *Bull. Eng. Geol. Environ.* 68 (2009) 525–537.
- [3] Geofizika Enterprize for Applied Geophysics, "Final Report, Southwestern Sinai, Reconnaissance Investigation: Hydrogeology, Geophysics, and Soil Studies. Zagrab" (1963)
- [4] U. Dayan, R. Abramski: "Heavy rain in the Middle East related to unusual jet stream properties. *BullAmMeteorol Soc* .64 (1983) 1138–1140.
- [5] K. Rina, C. K. Singh, P. S. Datta, N. Singh, S. Mukherjee, "Geochemical modelling, ionic ratio and GIS based mapping of groundwater salinity and assessment of governing processes in Northern Gujarat, India" *Environ Earth Sci.* 69 (2013) 2377–2391.
- [6] M. Chetia, S. Chatterjee, S. Banerjee, M. J. Nath, L. Singh, R. B. Srivastava, H. P. Sarma, "Groundwater arsenic contamination in Brahmaputra river basin: a water quality assessment in Golaghat (Assam), India" *Environ Monit Assess* 173 (2011) 371–385.
- [7] APHA, "Standard methods for the examination of water and wastewater" 21st edn. American Public Health Association, Washington DC. (2005).
- [8] H. Schoeller, "Geochemistry of groundwater. Groundwater studies—an international guide for research and practice Ch. 15. UNESCO, Paris, (1977) 1–18.
- [9] J. D. Hem, "Study and interpretation of the chemical characteristics of natural water" U.S. Geological Survey, water supply, Papers (1989) 1374 & 2254.
- [10] G. Han, C. Q. Liu, "Water geochemistry controlled by carbonate dissolution: a study of the river waters draining Karst-dominated terrain" *Guizhu Province. China chemical Geology*, 204 (2004) 1-21.
- [11] N. Aghazadeb, A.A. Mogaddam, "Assessment of groundwater quality and its suitability for drinking and agricultural uses in the Oshnavieh area, Northwest of Iran" *journal of environmental protection*, 1 (2010) 30-40.
- [12] M. Kumar, K. Kumari, A.L. Ramanathan, R. Saxena, "A comparative evaluation of groundwater suitability for irrigation and drinking purposes in two intensively cultivated districts of Punjab, India" *Environ Geol* 53 (2007) 553–574 Oxford & IBH Pub. Co., New Delhi.
- [13] S. Y. Acheampong, J. W. Hess, "Hydrogeological and hydrochemical framework of the shallow groundwater system in the southern Voltaian sedimentary basin, Ghana" *Hydrogeology Journal*, 6 (1998) 527-537.
- [14] S. M. Yidana, D. Ophori, B. Banoeng-Yakubo, "Groundwater availability in the shallow aquifers of the southern Voltaian system: a simulation and chemical analysis" *Environ Geol* 55 (2008) 1647–1657.
- [15] A. W. Hounslow, "Water quality data analysis and interpretation", New York, Lewis Publisher hydrogeochemical processes in the groundwater environment in an area of the Palar and Cheyyar River Basins, Southern India. *Environ Geol* 46 (1995) 47–61.
- [16] D. K. Todd, "Groundwater Hydrology" International Edition, John Wiley & Sons, Inc., New York (1959)
- [17] P.s. Datta, S. K. Bhattacharya, S.K. Tyagi, SK, "¹⁸O studies on recharge of phreatic aquifers and groundwater flow-paths of mixing in the Delhi area" *J Hydrol* 176 (1996) 25–36.
- [18] N. Rajmohan, L. Elango, "Identification and evolution of hydrogeochemical processes in the groundwater environment in an area of the Palar and Cheyyar River Basins, Southern India" *Environmental Geology* 46 (2004) 47-61.
- [19] M. M. Sarin, S. Krishnaswamy, K. Dilli, B.L.K. Somayajulu, W.S. Moore, "Major ion chemistry of the Ganga- Brahmaputra river system: weathering processes and fluxes to the Bay of Bengal" *Geochim Cosmochim Acta* 53 (1989) 997–1009.
- [20] P.S. Datta, S.K. Tyagi, "Major ion chemistry of groundwater of Delhi area: chemical weathering processes and groundwater flow regime" *J Geol Soc India* 47 (1996) 179–188.
- [21] N. S. Rao ' Factors controlling the salinity in groundwater in parts of Guntur district, Andhra Pradesh, India" *Environ Monit Assess* 138 (2008) 327–341.
- [22] N. S. Rao, "Seasonal variation of groundwater quality in a part of Guntur district, Andhra Pradesh, India. *Environ Geol* 49 (2006) 413–429.
- [23] W. M. Edmunds, J.J.C.-Rivera, A. Cardona, "Geochemical evolution of groundwater beneath Mexico City" *J Hydrol* 258 (2002) 1–24.

- [24] (WHO) World Health Organization, "Guidelines for drinking water. Quality" vol. 1. (2011) Recommendations. World Health Organization, Geneva, 130 pp.
- [25] I. I Chebotarev, "Metamorphism of natural waters in the crust of weathering. Geochim" Cosmochim. Acta, 8 (1955) 137-170 and 198 - 212, London, New York.
- [26] L. V. Wilcox, "Classification and use of irrigation waters". U.S.A., Salinity Lab. Circulation No.969 (1955) Washington D.C., U.S.A.
- [27] U.S Salinity Laboratory Staff, "Diagnosis and improvement of saline and alkali soils" Dep. Agric., Hand Book, Washington D.C., No.60 (1954) p.1-60.
- [28] I. I. M. Raghunath, "Groundwater Second edition" Wiley Eastern. Lth. New Delhi, India (1987) 344-369.
- [29] I. A. Richards, "Diagnosis and improvement of saline and alkali soils" United States department of Agriculture (USDA), Washington, USA, Handbook No. 60 (1954) 160.
- [30] S. K. Gupta, I. C. Gupta," Management of saline soils and waters" Oxford & IBH Pub. Co., New Delhi (1987).
- [31] I. Szabolcs, C. Darab, "The Influence of Irrigation Water of High Sodium Carbonate Content of Soils" Proceedings of 8th International Congress of ISSS, Trans II (1964) 803-812.
- [32] W.P. Kelley, "Permissible composition and concentration of irrigation waters". Proc ASCE, 66 (1940) 607.
- [33] S. K. Sundaray, B. B. Nayak and D. Bhatta, "Environmental studies on river water quality with reference to suitability for agricultural purposes: Mahanadi river estuarine system, India — a case study" Environ. Monitor Assess. 155 (2009) 227–243.